

See discussions, stats, and author profiles for this publication at: <https://www.researchgate.net/publication/244402107>

Electrooxidation of H₂/CO Mixtures on a Well-Characterized Pt₇₅Mo₂₅ Alloy Surface

ARTICLE in THE JOURNAL OF PHYSICAL CHEMISTRY B · MAY 1997

Impact Factor: 3.3 · DOI: 10.1021/jp9704168

CITATIONS

102

READS

29

4 AUTHORS, INCLUDING:



Branimir N. Grgur

Faculty of Technology and Metallurgy, Unive...

108 PUBLICATIONS 3,183 CITATIONS

SEE PROFILE



N. M. Marković

Argonne National Laboratory

285 PUBLICATIONS 21,900 CITATIONS

SEE PROFILE



Philip N Ross

University of California, Berkeley

360 PUBLICATIONS 21,340 CITATIONS

SEE PROFILE

Electrooxidation of H₂/CO Mixtures on a Well-Characterized Pt₇₅Mo₂₅ Alloy Surface

B. N. Grgur, G. Zhuang, N. M. Markovic, and P. N. Ross, Jr.*

Materials Sciences Division, Lawrence Berkeley National Laboratory, University of California, Berkeley, California 94720

Received: February 4, 1997; In Final Form: March 27, 1997[⊗]

The electrochemical oxidation of hydrogen in the presence of carbon monoxide (0.05–2%) on a well-characterized Pt₇₅Mo₂₅ alloy surface was examined using the rotating disk electrode technique in 0.5 M H₂SO₄ at 333 K. The surface composition of this alloy determined by low-energy ion scattering after sputter cleaning and annealing in UHV was essentially the same as the bulk. The shapes of the polarization curves are qualitatively similar to those for the Pt₅₀Ru₅₀ alloy examined previously: a high Tafel-slope (ca. 0.5 V/dec) region at low overpotential followed by a transition to a highly active state where the current approaches the diffusion-limiting current; the potential where the transition to the active state occurs decreases with decreasing CO concentration, and the current in the low-overpotential region is roughly inverse half-order in the CO partial pressure. The magnitude of the current in the low-overpotential region on the Pt₇₅Mo₂₅ alloy is nearly the same as on the Pt₅₀Ru₅₀ alloy, but the potential for the transition to the active state is about 0.15 V higher. The magnitude of the current at 0.05–0.1 V with H₂ containing 100 ppm CO is sufficiently high that Pt–Mo alloy is of technical interest as an anode catalyst for low-temperature fuel cells fed with a reformed hydrocarbon fuel.

Introduction

A major problem in the development of low-temperature fuel cells for transportation applications is the deactivation of the Pt anode catalyst by even trace levels, e.g. 10–100 ppm, of carbon monoxide (CO). The anode deactivation produced by low concentrations of CO necessitates the use of either pure hydrogen or an extensive purification system for hydrogen generated on board the vehicle by steam reforming a hydrocarbon fuel. A review of efforts to develop alternative catalysts that are tolerant to CO in hydrogen can be found in ref 1.

In recent studies,^{2–4} we investigated the oxidation of H₂, CO, and their mixtures on Pt, Ru, Pt–Ru alloys,^{2,3} and Pt₃Sn,^{1,4} all as solid electrodes prepared and characterized in UHV and transferred into a rotating disk electrode assembly for kinetic evaluation of the reaction rates. In the present Letter, we report results for the electrooxidation of H₂ and H₂/CO mixtures on a solid solution Pt₇₅Mo₂₅ alloy using identical methodology. The characteristics of the Pt₇₅Mo₂₅ surface for the oxidation of H₂/CO mixtures are found to be remarkably similar to those of Pt₅₀Ru₅₀ alloy, which is surprising and interesting in view of the seemingly disparate chemistry of Ru and Mo.

Experimental Section

The polycrystalline Pt–Mo alloy was prepared as bulk crystal by arc melting of the pure elements in an argon atmosphere and a homogenizing heat treatment. Details of the preparation procedure, which was the same as used for Pt–Ru alloys, are given in ref 2. The nominal composition of the alloy from the weight of the pure metals was 25.0 at. % Mo. X-ray diffraction analysis confirmed the formation of a single-phase fcc structure with lattice constant 0.3098 nm, in agreement with the lattice constant given for the Pt solid solution alloy with 20 ± 5 at. % Mo in Pearson.⁵ The alloy boule was precision ground into a cylinder shape to fit into a Pine Instruments insertable rotating disk electrode (RDE) arbor.⁶

Low-energy ion scattering (LEIS) and Auger electron spectroscopy (AES) data were collected using a angle-resolving double-pass cylindrical mirror analyzer. Details of the data collection procedure were reported previously.⁷ For LEIS, a 2 keV ⁴He⁺ ion beam was rastered over a 3 mm × 3 mm area of the surface at an incident angle of 45°. The average scattering angle was 127° with resolution less than 1°. Calibration of LEIS intensities was carried out using pure Pt and Mo polycrystals.

All data reported here were obtained using the alloy sample inserted into a Pine RDE arbor following cleaning and characterization in UHV. The detailed procedure for the transfer from UHV and insertion into the RDE has been given previously.⁸ The procedures for measuring hydrogen oxidation current–potential curves with the Pt–Mo alloy were the same as used previously for Pt–Ru alloys, and the details are given in refs 2 and 3. All potentials given here are referred to the reversible hydrogen electrode (RHE) at the same temperature.

Results and Discussion

AES analysis was conducted only for the purposes of assessing surface cleanliness. A typical AES spectrum for the Pt–Mo alloy surface after numerous cycles of Ar ion sputtering (0.5 keV) and thermal annealing (973 K for 30 min) is shown in Figure 1. It did not appear practical to remove all traces of carbon and oxygen from the annealed surface; while the sputtered surface showed carbon and oxygen detectable by AES, they reappear on the thermal annealing cycle, probably by surface segregation from the bulk. The trace amounts remaining, however, were considered not to affect the LEIS analysis or the electrochemical properties of the surface. A typical LEIS spectrum from this surface is shown in the inset in Figure 1. The peak energies for Pt and Mo agreed to within ±0.5% with the values predicted by the classical equation for elastic collisions.⁹ The surface composition was calculated from the peak heights, *H*_{Pt} and *H*_{Mo}, determined by fitting the spectrum with Gaussian profiles and correcting for the inelastic background,⁷ according to

* Corresponding author: phone, (510) 486-6226; fax, (510) 486-5530; e-mail, pnross@lbl.gov.

[⊗] Abstract published in *Advance ACS Abstracts*, May 1, 1997.

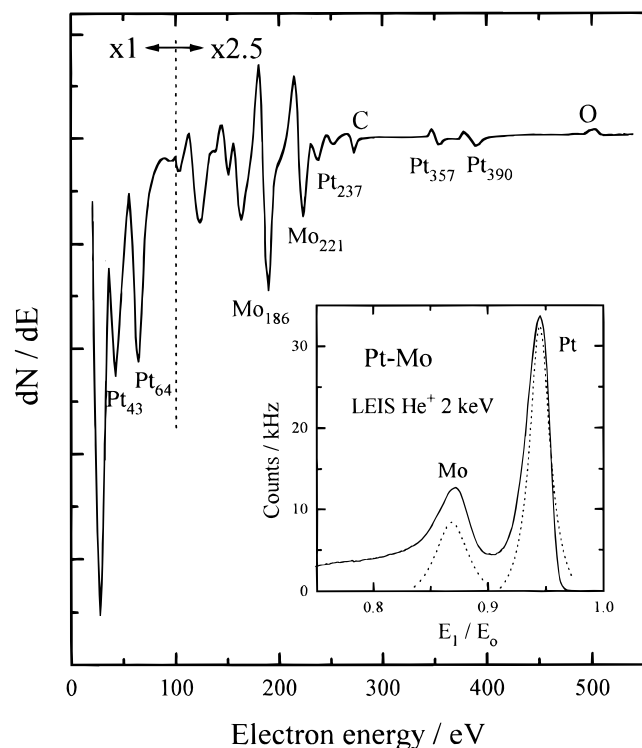


Figure 1. Derivative mode AES spectrum of the $\text{Pt}_{75}\text{Mo}_{25}$ alloy following sputter cleaning and annealing at 970 K. (inset) LEIS spectrum of the same surface (dashed curve is fitted spectrum after subtraction of the inelastic tail⁷).

$$X_{\text{Mo}} = S_{\text{Mo/Pt}} / [S_{\text{Mo/Pt}} + (H_{\text{Mo}}/H_{\text{Pt}})_{\text{exp}}]$$

where $S_{\text{Mo/Pt}}$ is the empirical sensitivity for Mo relative to Pt. The empirical sensitivity factor was determined from the peak heights in the pure samples according to¹⁰

$$S_{\text{Mo/Pt}} = (H_{\text{Mo}}/H_{\text{Pt}})_{\text{pure}} (a_{\text{Pt}}/a_{\text{Mo}})^2$$

where a_{Pt} and a_{Mo} are the lattice constants for the pure metals. The resulting surface composition from the spectrum in Figure 1 for the annealed surface was 23 at. % Mo. This result indicates there is little or no enrichment of the surface in Pt, contrary to the predictions of thermodynamic models.¹¹ It is possible that the annealing of the Pt–Mo alloy at the relatively low temperature of 973 K does not produce an equilibrated surface. Due to preferential sputtering of Pt, the sputter-cleaned surface was Pt deficient; annealing restores the surface to near the bulk composition, and it is possible higher temperature and/or longer annealing would have produced the Pt-enriched surface predicted in thermodynamic models.

The stability of Mo in the surface in 0.5 M H_2SO_4 was examined by removing the electrode from the cell, washing with water, and reinsertion into the UHV chamber for analysis by LEIS. Although contamination of the surface by impurities from the transfer were obvious, e.g. mostly carbon and oxygen, both LEIS and AES peaks from Pt and Mo were observable and quantifiable and indicated no loss of Mo from the surface as a result of electrochemical examination, which included repeated cycling at various sweep rates from 0. to 0.8 V.

The voltammetry of the $\text{Pt}_{75}\text{Mo}_{25}$ surface in argon-purged electrolyte and the slow sweep (1 mV/s) current–potential curve for H_2 oxidation are shown in Figure 2. In spite of the fact that the surface is only 23 at. % Mo, the voltammetry has very little Pt character, having no distinct peaks for hydrogen adsorption/desorption in the 0–0.3 V region, and very large

pseudocapacitance in the 0.3–0.6 V region. The absence of distinct hydrogen adsorption/desorption peaks is similar to the character of the Pt_3Sn surface,⁴ but the large pseudocapacitance more resembles the character of the $\text{Pt}_{50}\text{Ru}_{50}$ surface.¹² As described below, this mixed character of the $\text{Pt}_{75}\text{Mo}_{25}$ is a recurrent theme which emerged from this preliminary study. As with $\text{Pt}_{50}\text{Ru}_{50}$, the large pseudocapacitance is probably due to OH_{ads} formation on the Mo surface atoms and/or redox processes on oxidized Mo surface atoms. The voltammetry curves were unaffected by cycling in the potential region shown, the first cycle upon transfer from UHV being identical to the n th cycle. This is further evidence of the stability of Mo in the surface.

The kinetics of oxidation of pure H_2 on the $\text{Pt}_{75}\text{Mo}_{25}$ surface is indistinguishable from that on the pure Pt surface.² The overpotential/current relation, shown in the inset, at the rotation rates used here closely follows that for pure diffusion control¹²

$$\eta = -(RT/2F) \ln(1 - i/i_d)$$

where i_d is the measured diffusion-limited current at any rotation rate, i is the observed current density at the overpotential η , and R , T , and F have their usual meaning (at 333 K, $RT/2F$ is 33 mV/decade). (Since we are using a hydrogen electrode as the reference electrode, the overpotential for the oxidation of hydrogen, η , is equal to the electrode potential, E .) Because the rate of reaction is so high on either the pure Pt or the Pt–Mo alloy surface relative to the rate of H_2 transport possible with the RDE, it is impossible to say whether or not there is a kinetic difference between the two surfaces.

The polarization curves for the oxidation of H_2 in the presence of CO (2, 0.1, and 0.05 vol %) at 333 K are shown in Figure 3. The curves are recorded on the anodic sweep (1 mV) from 0 V after switching from pure H_2 to the H_2/CO mixture and waiting for 10 min. Quasi-steady state (15 min) currents recorded using potential steps from 0 V were not significantly different from the curves shown. The shapes of these polarization curves are qualitatively similar to those for the $\text{Pt}_{50}\text{Ru}_{50}$ alloy:³ there is a high Tafel-slope (ca. 0.5 V/decade) region at low overpotential followed by a transition to a highly active state where the current approaches the diffusion-limiting current; the potential where the transition to the active state occurs decreases with decreasing CO concentration, and the current in the low-overpotential region is roughly inverse half-order in the CO partial pressure (inset). The magnitude of the current in the Tafel region is nearly the same on the $\text{Pt}_{75}\text{Mo}_{25}$ alloy versus $\text{Pt}_{50}\text{Ru}_{50}$ alloy, but, as the comparison in Figure 4 for 0.1% CO clearly shows, the potential for the transition to the active state is lower by about 0.15 V, and the transition is much sharper for the $\text{Pt}_{50}\text{Ru}_{50}$ alloy. The transition to the diffusion-limiting current on $\text{Pt}_{75}\text{Mo}_{25}$ occurs at about 0.1 V lower potential than on pure Pt. Since we had shown previously^{2,3} that the transition to the highly active state on both Pt and Pt–Ru alloys occurs at the potential where the CO starts to be oxidized at a high rate, e.g. one-half the diffusion-limited rate, the differences in transition potential between Pt–Mo alloy and pure Pt and Pt–Ru alloy surfaces imply that CO oxidation on Pt–Mo begins at about 0.2 V higher than on $\text{Pt}_{50}\text{Ru}_{50}$ and at only slightly lower potential than on pure Pt. Confirmation of this expectation is found in the polarization curve for 2% CO in argon shown in the upper inset of Figure 3, where the transition to the diffusion-limiting current occurs in the same potential region as for $\text{H}_2/2\%$ CO (with about a 50-fold lower limiting current, not shown).

The magnitude of the current in the potential region 0.05–0.1 V with H_2/CO mixtures of 0.1% CO and lower has significance for fuel cell technology. Using established conver-

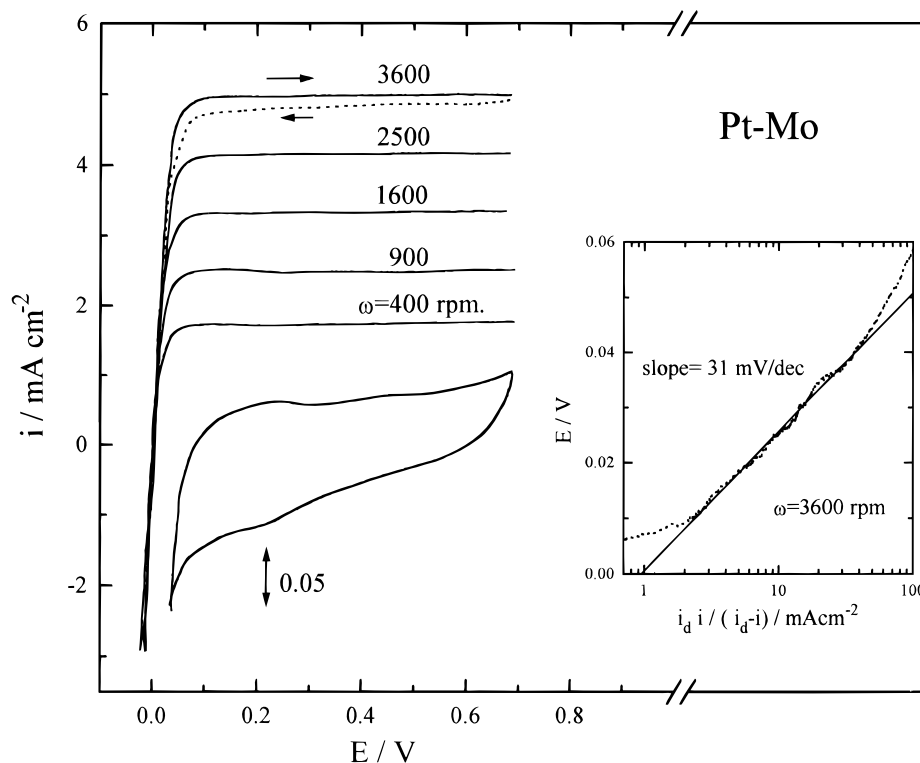


Figure 2. (lower) Cyclic voltammogram in deaerated electrolyte for the Pt₇₅Mo₂₅ alloy following transfer from UHV; 50 mV s⁻¹, 0.5 M H₂SO₄ at 333 K. (upper) Current–potential curves in H₂-saturated electrolyte at 333 K; 1 mV s⁻¹. (inset) Tafel plot of the current–potential curve for H₂ oxidation at 3600 rpm.

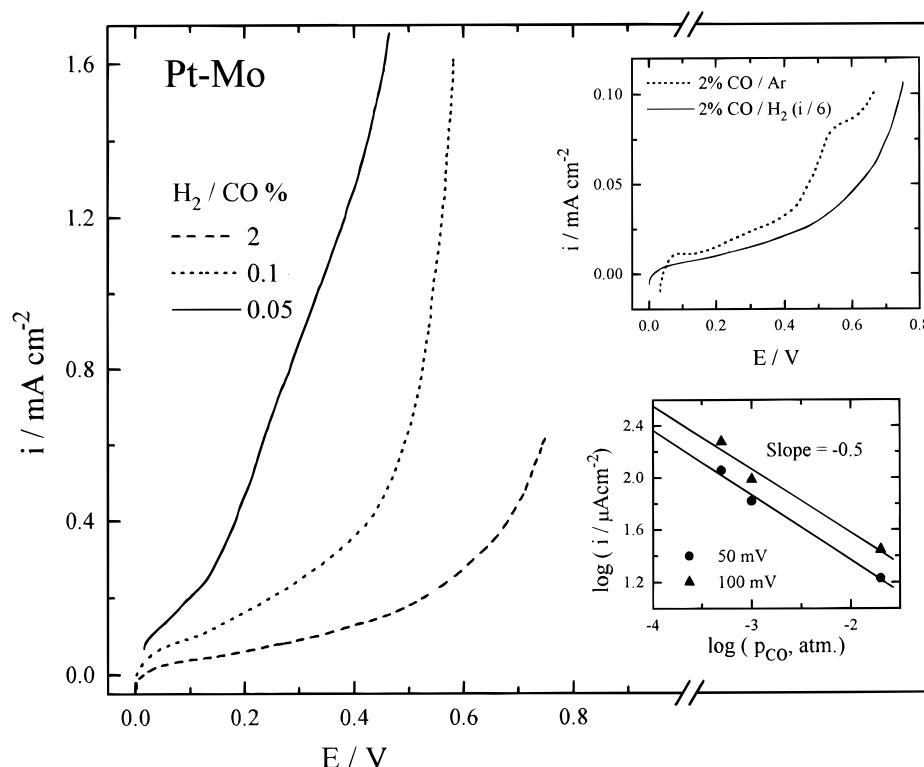


Figure 3. (left) Current–potential curve for the oxidation of H₂ on Pt₇₅Mo₂₅ alloy containing various levels of CO at 2500 rpm; 1 mV s⁻¹, 333 K. (inset, upper) Current–potential curve for oxidation of H₂/2% CO versus 2% CO/argon mixture at 2500 rpm. (inset, lower) Reaction-order (in CO) plot for H₂/CO mixtures in the low-potential region.

sion factors based on experience, it is possible to establish a target current density with solid electrodes that would be expected to produce acceptable current densities in working fuel cell anodes.¹³ This target current density is 0.2 mA cm⁻², which the data in Figure 3 (inset) shows would be achievable with a Pt₇₅Mo₂₅ alloy catalyst with CO levels of 100 ppm. The Pt₅₀-

Ru₅₀ alloy has comparable activity to Pt₇₅Mo₂₅ for H₂/CO mixtures in our study, and we note that a supported Pt–Ru alloy (50% Ru) catalyst is reported to provide acceptable activity in a polymer electrolyte membrane (PEM) fuel cell with H₂ containing 100 ppm CO.¹⁴

The mechanism of the activity enhancement of Pt₇₅Mo₂₅

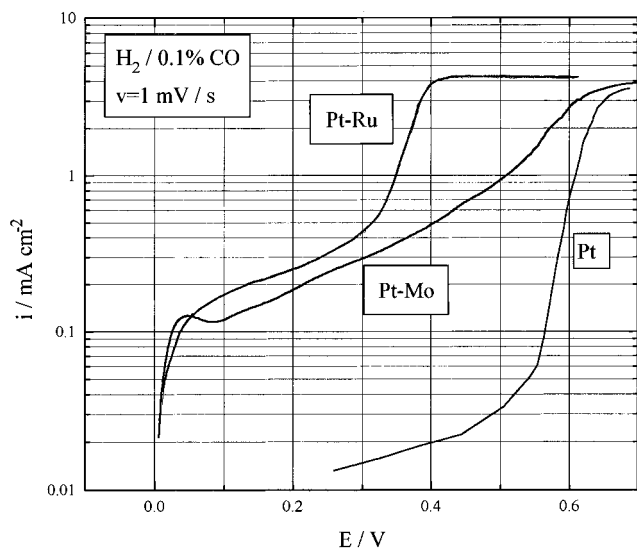


Figure 4. Log i versus potential curves recorded on anodic sweep at 1 mV s^{-1} for oxidation of $\text{H}_2/0.1\% \text{ CO}$ on pure Pt, $\text{Pt}_{50}\text{Ru}_{50}$, and $\text{Pt}_{75}\text{Mo}_{25}$ surfaces following identical protocols.

versus pure Pt for the oxidation of H_2/CO mixtures at 0.05–0.1 V is not obvious and is of considerable fundamental interest. In the case of the $\text{Pt}_{50}\text{Ru}_{50}$ alloy surface, we have shown that the current in this potential region, which is about 20 times higher than with pure Pt, H_2 is being oxidized on a surface covered by CO at or near saturation coverage.³ We suggested that the higher residual current originates from “holes” in the CO monolayer on Pt–Ru alloy in contrast to the essentially perfect CO adlayer on Pt. It is useful to demonstrate how the presence of a very small number of free, unpoisoned Pt sites is “magnified” by H_2 oxidation. Consider a simple site-blocking model¹⁵ for the poisoning of H_2 oxidation by adsorbed CO, given by

$$i_{\text{CO}} = i_{\text{H}_2}(1 - \Theta_{\text{CO}})^2$$

where i_{CO} is the current in the presence of CO, i_{H_2} is the current for pure H_2 , and Θ_{CO} is the CO_{ads} coverage, all at a given potential. For demonstration purposes, consider that on pure Pt Θ_{CO} is 0.98, and on Pt–Ru alloy the coverage is slightly less, 0.93. This difference in coverage of 5% is essentially unmeasurable on polycrystalline surfaces but produces in this model a factor of 12 in current, the same order of magnitude difference we observe here. Possibly a similar perturbation in the “CO carpet” on the Pt sites is produced by the presence of Mo in the surface at ca. 25 at. %, but another mechanism of action is highly likely. An indication that this is the case may be seen in the current–potential curve for 2% CO in argon (inset, Figure 3), which is about five times higher in the 0.05–0.2 V region on $\text{Pt}_{75}\text{Mo}_{25}$ than on $\text{Pt}_{50}\text{Ru}_{50}$. This higher rate of oxidation of CO, still far below the diffusion-limiting current for 2% CO, implies a more complex chemistry is at work on

the $\text{Pt}_{75}\text{Mo}_{25}$ surface. Furthermore, the surface chemistry and electrochemistry of Mo and Ru seem too disparate to function in the same way, although the alloying with Pt can change the chemistry of the admetal in dramatic and unpredictable ways. Ru is a Pt-group metal and shares the common property of these metals that it adsorbs both hydrogen and CO, has quasi-reversible OH_{ads} states in a limited potential region, e.g. 0–0.8 V, and is an electrocatalyst for both H_2 oxidation and CO oxidation, actually being more active than pure Pt for the latter.² These chemical properties appear to be preserved when Ru is alloyed with Pt.^{3,10} The electrochemistry of Mo is very different; its surface in dilute ($\text{pH} > 2$) acid solution is covered by a tetravalent oxide, but it dissolves in strong acids ($\text{pH} < 1$) at potentials above -0.2 V and has a very large hydrogen overpotential.¹⁶ However, the fact that Mo is not dissolved from the alloy surface at potentials up to 0.8 V indicates that the intermetallic bonding with Pt is significant and changes at least some of its intrinsic chemical properties. In that sense, $\text{Pt}_{75}\text{Mo}_{25}$ is like Pt_{3}Sn , where the intermetallic bonding is known to be very strong¹⁷ and stabilizes Sn in the surface. $\text{Pt}_{75}\text{Mo}_{25}$ is, therefore, a surface with unexpected electrocatalytic properties of both technical and fundamental interest deserving further consideration and study.

Acknowledgment. This work was supported by the Assistant Secretary for Energy Efficiency and Renewable Energy, Office of Transportation Technology, of the U.S. Department of Energy under contract number DE-AC03-76SF00098.

References and Notes

- Gasteiger, H.; Markovic, N.; Ross, P. *J. Phys. Chem.* **1995**, *99*, 8945.
- Gasteiger, H.; Markovic, N.; Ross, P. *J. Phys. Chem.* **1995**, *99*, 8290.
- Gasteiger, H.; Markovic, N.; Ross, P. *J. Phys. Chem.* **1995**, *99*, 16757.
- Markovic, N.; Ross, P. *Catal. Lett.* **1996**, *36*, 1.
- Pearson, W. In *A Handbook of Lattice Spacings and Structures of Metals and Alloys*; Pergamon Press: Oxford, UK, 1958; p 755.
- Pine Instrument Company, 101 Industrial Drive, Grove City, PA 16127.
- Gasteiger, H.; Ross, P.; Cairns, E. *Surf. Sci.* **1993**, *293*, 67.
- Markovic, N.; Gasteiger, H.; Ross, P. *J. Phys. Chem.* **1995**, *99*, 3411.
- Riviere, J. *Surface Analytical Techniques*; Oxford University Press: Oxford, UK, 1990.
- Baun, W. In *Quantitative Surface Analysis of Materials*; ASTM STP 643; McIntyre, N. S., Ed.; American Society for Testing and Materials, Philadelphia, PA, 1978; p 150.
- Mukherjee, S.; Moran-Lopez, J. *Surf. Sci.* **1987**, *189/190*, 1135.
- Gasteiger, H.; Markovic, N.; Ross, P.; Cairns, E. *J. Phys. Chem.* **1994**, *98*, 617.
- Gasteiger, H.; Markovic, N.; Ross, P.; Cairns, E. *J. Electrochem. Soc.* **1994**, *141*, 1795.
- Oetjen, H.-F.; Schmidt, V.; Stimming, U.; Trila, F. *J. Electrochem. Soc.* **1996**, *143*, 3838.
- Vogel, W.; Lundquist, J.; Ross, P.; Stonehart, P. *J. Electroanal. Chem.* **1975**, *20*, 79.
- Pourbaix, M. *Atlas of Electrochemical Equilibria in Aqueous Solutions*; Pergamon Press: London, UK, 1966; pp 272–79.
- Ross, P. *J. Vac. Sci. Technol. A* **1992**, *10*, 2546.